Research Square

Preprints are preliminary reports that have not undergone peer review.
They should not be considered conclusive, used to inform clinical practice,
or referenced by the media as validated information.

Catalytic degradation of Methylene blue by Biosynthesized Au Nanoparticles on titanium dioxide (Au@TiO2)

Yanan Wang
Agro-Environmental Protection Institute
Tieliang Zhang
Agro-Environmental Protection Institute
Yujie Zhao
Agro-Environmental Protection Institute
Tong Lv
Agro-Environmental Protection Institute
Wenjing liu (liuwenjing@caas.cn)
Agro-Environmental Protection Institute https://orcid.org/0000-0002-7559-5606
Xiaowei Liu
Agro-Environmental Protection Institute

Research Article

Keywords: Biosynthesis, Au NPs@TiO2, Methylene blue, Catalytic degradation

Posted Date: June 27th, 2022

DOI: https://doi.org/10.21203/rs.3.rs-1756688/v1

License: This work is licensed under a Creative Commons Attribution 4.0 International License.
Read Full License

Abstract

Degradation of methylene blue is a critical procedure in its wastewater remediation, thus has inspired wide catalysis research with semiconductors such as Titanium dioxide (TiO_2) and rare metals such as gold (Au). In this study we report bacterial cells assisting biosynthesis for Au@TiO_2 as an efficient catalyst for the degradation of methylene blue. Multiple complementary characterization for bio-Au_x@TiO_2 evidenced the evenly distributed Au NPs on the bio-TiO_2 layers. Meanwhile, bio-Au_2@TiO_2 displayed the superior catalytic activity in the degradation of methylene blue with the highest k value of 0.195 min^{-1}. The origin of the catalytic activity was explored by the hydroxyl radical fluorescence quantitative analysis. In the bio-Au_2@TiO_2 catalytic system, Au NPs decreased the band gap energy of TiO_2, increased charge separation between the excited (h^+)–(e^-) pairs, enabling the generation of a large amount of photogeneration hydroxyl radicals, resulting in an enhanced photocatalytic activity. Our microbial synthesized bio-TiO_2 and bio-Au_x@TiO_2 study would be useful for developing green synthesis catalyst technologies.

1. Introduction

The elimination of organic pollutants from wastewater is a major challenge for the ecosystem.(Cai et al. 2022, Lee et al. 2016) Due to their synthetic origin and aromatic nature, azo dyes are stable, nonbiodegradable, and carcinogenic. (Routoula &Patwardhan 2020) Even microquantities of these dyes lead to acute toxicity in aquatic life, and thus pose a health risk to human vis the food chain.(de Luna et al. 2014) In this case, photocatalytic degradation of dye molecules (methylene blue) is an efficient and feasible treatment method for wastewater.(Miranda et al. 2015, Saeed et al. 2022)

Titanium dioxide (TiO_2) is widely applied in environmental remediation owing to its non-toxicity, chemical stability, high photocatalytic activity and recyclability.(Chong et al. 2010, Forgacs et al. 2004) TiO_2 materials were most commonly used photo-catalyst and have been successfully employed in the degradation of organic contaminants.(Chen et al. 2010, Pelaez et al. 2012) However, TiO_2 can only be excited in the UV region (200–400 nm) because of its wide band gap (3.0 ~ 3.2 eV). (Chen &Mao 2007) Photogenerated electron-hole recombination rate of pristine TiO_2 was high, resulted in decreased catalytic activity. It was found that loading noble metal nanoparticles (Ag, Au, Pt, and Pd) with surface plasmon resonance effect could effectively enhance the optical absorption and accelerate the interfacial charge transfer.(Kochuveedu et al. 2013, Sarina et al. 2013, Zhang et al. 2012)

Au nanoparticles (Au NPs) are one of the most promising and widely used materials in a variety of heterogeneous catalytic reactions.(Liu &Corma 2018) The Several applications of Au/TiO_2 nanocomposite have been reported in the photocatalytic removal and degradation of dyes, including methylene blue, orange 16, sulforhodamine-B, and tartazine under visible or UV light.(Angthararuk et al. 2015, Ayati et al. 2014) A laser flash photolysis study of Au-capped TiO_2 demonstrated an increase of 40% in hole transfer efficiency.(Dawson &Kamat 2001) It has been observed that the photocatalytic

activity of Au/TiO_2 materials was higher than that of Au nanoparticles or pure TiO_2 materials. (Liu et al. 2013)

Hence, it has attracted great attention to synthesize Au@TiO_2 nanocomposite materials with outstanding catalytic properties.(Alsaidi et al. 2022, Green et al. 2014) Due to its low-cost, eco-friendliness, and mild synthetic environment, the microorganism-assisted green synthesis is considered as an alternative to synthesizing composite materials.(Bhargava et al. 2016, Dahl et al. 2007, Nasrollahzadeh &Sajadi 2016, Nasrollahzadeh et al. 2020, Singh et al. 2016) Several microorganisms, notably bacteria, have been investigated for synthesizing Au NPs.(Reith et al. 2006, Sahu et al. 2022, Sanyal et al. 2019, Southam et al. 2009) Previous studies have shown that *Pantoea* sp. IMH, a strain that has multiple metal resistance genes, (Liu et al. 2018b) was able to reduce Au(III) to form Au NPs.(Liu et al. 2018a) Consequently, earlier results inspired us to synthesize Au@TiO_2 nanocatalyst by employing biomineralized Au NPs.

In this study, we proposed a green synthesis method for Au@TiO_2 using strain IMH. Multiple complementary methods were utilized to characterize the biosynthesized Au@TiO_2. Au@TiO_2 was employed in the catalytic degradation of methylene blue. In addition, hydroxyl radicals formed in the degradation reaction were quantitatively analyzed to explore the catalytic mechanism of Au@TiO_2. The insights obtained from our work enhance the deep understanding on the microbial synthesis and mechanism of TiO_2-based environmental technologies.

2. Experimental

2.1 Materials

All chemicals, containing chloroauric acid tetra hydrate ($HAuCl_4 \cdot 4H_2O$) and methylene blue trihydrate ($C_{16}H_{24}ClN_3O_3S$) were obtained from Sinopharm Chemical Reagent Co., Ltd (China). Microbiological medium ingredients were bought from Oxoid Co., Ltd (England). Titanic acid ($TiO(OH)_2$) was acquired from Beijing Ouhe Technology Co., Ltd (China). Ultrapure Milli-Q water (18.2 MΩ) was used in all experiments.

2.2 Bacterial Strains and Culture Conditions

Pantoea sp. IMH (JX861130) was cultured in Luria – Bertani (LB) broth at 30 ^oC. Bacterial cells were incubated to late-exponential phase at 160 rpm for 8 h on a rotary shaker. Cells were harvested by centrifugation at 4000 *g* for 5 min and were washed three times with phosphate-buffered saline (PBS buffer). Then the harvested cells were re-suspended and incubated in PBS buffer.

2.3 Synthesis of bio-TiO_2 and bio-Au_x@TiO_2

A 3 mM, 100 mL $TiO(OH)_2$ solution was prepared and stirred in a water bath (60 ^oC, 1 h). After the $TiO(OH)_2$ solution was cooled to room temperature, the above cell suspension (10 mL) was mixed with

$TiO(OH)_2$ solution at 30 ^oC for 3 h. The resulting bacterial suspension was centrifuged at 8000 *g* for 10 min, and washed thoroughly with sterile water. The obtained precipitated solid substance was dried in vacuum (60 ^oC, 2 h) and then calcined in a tube furnace at 400 ^oC for 2 h to get TiO_2 (namely, Bio-TiO_2). Meanwhile, partial reaction production suspension without drying treatment was used in the next step. In addition, commercial Titanium dioxide (TiO_2, P25) particles as control sample were obtained from Beijing Baoruyi Biotechnology Co., Ltd (China).

The above TiO_2 suspension was further mixed with the cell suspension (10 mL). Then, Au(III) was added to a final concentration of 0.5 mM, 0.75 mM, 1 mM, and 2 mM, respectively. The mixtures were incubated at 30°C for 5 h. Then, the resulting suspension was centrifuged at 8000 *rpm* for 10 min, and the precipitate was washed with sterile water. And the products was dried (60 ^oC, 2 h) and then calcined (400 ^oC, 2 h) to get Au/TiO_2 (namely, Bio-Au_x@TiO_2, where x is the final concentration of Au(III) in the solution).

2.4 Characterization

X-ray diffraction (XRD) technology was used to analyze the crystal structure of the obtained materials with Rigaku D/Max-2500 diffractometer (Netherlands). The powder samples were mounted on aluminum stubs using a double-sticky tape and analyzed with field emission scanning electron microscopy (FESEM) with an Oxford energy dispersive X-rayspectroscopy (EDS) analyzer (SU 8020, Hitachi). The high-resolution transmission electron microscopy (HRTEM) and EDX elemental mapping of the samples were carried out with a FEI Tecnai G^2 F20 instrument. X-ray photoelectron spectroscopy (XPS) spectra were obtained on an ESCALab 250Xi spectrometer (Thermo Scientific). Infrared spectra were collected by a Thermo-Nicolet Nexus 6700 FTIR spectrometer using 256 scans and a 4 cm^{-1} spectral resolution.

2.5 Catalytic degradation of Methylene blue

Catalytic degradation of methylene blue experiments was conducted in an Erlenmeyer flask with 0.0375 mM methylene blue in a suspension (50 mL) containing 30 mg bio-TiO_2 and bio-Au_x@TiO_2. The samples were firstly stirred in the dark for 3 h to achieve adsorption equilibrium. Then A mercury UV lamp (CEL-M500, wavelength 275 nm) was used as the light source. UV-vis spectra of the reaction solutions at different times were acquired using a UV-2450 spectrophotometer (Shimadzu, Japan) to record the catalytic degradation progress.

2.6 Fluorescence analysis

The measurement of OH radical was detected by the fluorescence probe (terephthalic acid) method on a FLS-1000 fluorescence spectrometer (Edingurgh Instruments, UK) with an excitation wavelength at 312 nm. (Nakabayashi &Nosaka 2015) Terephthalic acid (TA) could readily react with OH radical to form 2-hydroxy terephthalic acid (TAOH), which emits a fluorescence light at 426 nm. Before irradiation, the 50 mL mixed suspension including 1 mM TA and 30 mg of bio-TiO_2/bio-Au_x@TiO_2 was magnetically stirred in the dark for 3 h to establish the adsorption-desorption equilibrium. The light irradiation and sampling conditions were the same as those in catalytic degradation experiments.

3. Results And Discussion

3.1 Materials Characterization

The morphology and structure of bio-TiO_2 and bio-Au_x@TiO_2 materials synthesized by the IMH strain were characterized using multiple complementary techniques. XRD spectra (Fig. 1) resolved the characteristic diffraction peaks for bio-TiO_2 at 25.33°, 37.53°, 47.87°, 53.53°, 54.86°, 62.36° and 74.63°, corresponding to (101), (004), (200), (105), (211), (204) and (215) crystal planes of the standard anatase TiO_2 (JCPDS-01-071-1168), respectively.(Nassar et al. 2017) In the XRD spectra of bio-Au_x@TiO_2, the diffraction peaks at 38.19°, 44.39°, 64.58°, 77.57° and 81.73° correspond to the (111), (200), (220), (311) and (222) crystallographic planes of standard Au metal (JCPDS-01-089-3697), respectively.(Tran et al. 2022) And other major peaks from bio-Au_x@TiO_2 spectra corresponded to the planes of standard anatase (JCPDS-01-071-1168). (Nassar et al. 2017) In addition, the peak positions of TiO_2 did not shift from bio-TiO_2 to bio-Au_x@TiO_2, indicating that bio-TiO_2 still kept the anatase crystalline phase during the deposition of Au NPs. XRD spectra results demonstrated that the IMH strain could successfully synthesize bio-TiO_2 and bio-Au_x@TiO_2 materials.

The FE-SEM (Fig. 2a) micrograph and EDX spectrum showed that bio-TiO_2 consists of aggregated irregular spheres with diameters of about 50–100 nm. The SEM images (Fig. 2b-2e) of bio-Au_x@TiO_2 exhibited the Au NPs as bright dots were dispersed on the surface of bio-TiO_2 support. Meanwhile, the Au NPs of bio-$Au_{0.5}$@TiO_2 and bio-$Au_{0.75}$@TiO_2 were spheres with particle size of 5 ~ 10 nm; the diameter of Au NPs in bio-Au_1@TiO_2 was mainly 10 nm; and the Au NPs of bio-Au_2@TiO_2 were spheres with a diameter of 5 ~ 15 nm. With the increase of concentration of Au ions in cell solution, the quantity and dimension of biosynthesized Au NPs notably increased, and the nanoparticles distribution tends to be even.

HR-TEM in Figure S1 showed that Au NPs (5–20 nm) were evenly dispersed in the bio-TiO_2 layers. The EDS elemental mapping in Figure S1c shown that the bio-Au_2@TiO_2 nanocomposite synthesized by the IMH strain consisted of elemental Au, Ti, O, and C.

The valence state of Au and Ti in bio-Au_x@TiO_2 was analyzed using XPS as shown in Fig. 3. Specifically, the peaks at 83.7 ~ 84.4 eV and 87.4 ~ 87.9 eV were ascribed to the $4f_{7/2}$ and $4f_{5/2}$ of Au(0), respectively(Liang et al. 2012). XPS results further confirmed that the IMH strain could completely reduce Au(III) to synthesize Au NPs. The high resolution XPS scan resolved two peaks of Ti 2 p electrons at 459.3 eV and 465.05 eV, which were respectively assigned to Ti $2p_{3/2}$ and Ti $2p_{1/2}$ of oxidized state Ti^{4+}, respectively.(Khalid et al. 2016) The energy difference (5.7 eV) between the peaks of Ti $2p_{3/2}$ and Ti $2p_{1/2}$ is corresponding to the Ti^{4+} state of anatase phase TiO_2, which is consistent with the previous XRD results.(Trino et al. 2018)

The FTIR spectra of the IMH strain, bio-TiO_2 and bio-Au_x@TiO_2 were shown in Figure S2. The IMH strain spectra displayed typical bacterial characteristic peaks, which were mainly located at 3310 cm^{-1} (-OH stretching), 1610 cm^{-1} (C = C stretching), 1540 cm^{-1} (N-H bending) and 1040 cm^{-1} (C-N stretching). (Bosch et al. 2008, Fischer et al. 2006, Schmitt &Flemming 1998) While in the FTIR spectra of bio-TiO_2 and bio-Au_x@TiO_2, the broad band around 1000 cm^{-1} represented the stretching vibration of Ti-O-Ti bond.(Li et al. 2022) Meanwhile, the bands at 3310 cm^{-1} and 1610 cm^{-1}, which were ascribed to -OH group and C = C bond stretching, were also appeared in the spectra of bio-TiO_2 and bio-Au_x@TiO_2. Combined with previous literature,(Ni et al. 2021) the hydroxyl functional groups in IMH strain were speculated to react with metatitanic acid to dehydrate, and finally to produce bio-TiO_2.

Our previous research reported that the strain IMH used diverse strategies to reduce Au(III) to Au NPs(Lengke et al. 2006, Liu et al. 2018a), including reduction of Au(III) by exopolysaccharides in extracellular polymeric substances (EPS) and protein/enzymatic reduction in the cytoplasm involving *fucO* and glutathione relevant proteins.(Liu et al. 2018b) In this work, cells reduce Au(III) to form AuNPs and then AuNPs were deposited on the surface of bio-TiO_2, thus successfully synthesizing bio-Au_x@TiO_2.

3.2 Catalytic performance

The bio-TiO_2 and bio-Au_x@TiO_2 materials were applied to the degradation of methylene blue. After adding the bio-TiO_2 and bio-Au_x@TiO_2 materials, the absorbance at 664.5 nm (Abs664.5 nm) indicative of methylene blue decreased.(Zou et al. 2016) As shown in Fig. 4a, the bio-TiO_2 degraded 79% of methylene blue molecules within 60 mins, but the degradation does not continue with the further increase of reaction time to 90 mins. Increasing concentrations of Au(III) in bio-Au_x@TiO_2 from 0.5, 0.75, 1, to 2 mM bleached the blue color of the methylene blue in 50, 50, 40, and 30 min, respectively, indicating the completion of the reaction. For a quantitative comparison of kinetics, the first-order kinetics rate constant *kapp* was calculated to evaluate the catalytic activity of bio-TiO_2-relevant materials. Among others, bio-Au_2@TiO_2 exhibited highest degradation efficiency on methylene blue with the highest *kapp* (0.195 min^{-1}) (Fig. 4f). Meanwhile, bio-TiO_2 and other bio-Au_x@TiO_2 materials also have good photocatalytic degradation effect on methylene blue. And the degradation effect is directly proportional to the loading contents of Au in bio-Au_x@TiO_2 system.

Moreover, compared with Au@TiO_2-containing catalysts synthesized by chemical or biological methods reported in the previous literature (Table S2), the bio-Au_x@TiO_2 material, particularly bio-Au_2@TiO_2 had comparable or even higher catalytic performance in the degradation of methylene blue.

3.3 Hydroxyl Radical analysis

Highly reactive oxygen species, especially hydroxyl radical (•OH), plays a vital role in the organic pollutants degradation procedure in TiO_2/UV system. To evaluate the content of ·OH in our study, the terephthalic acid (TA) fluorescent probe method was employed.(Nakabayashi &Nosaka 2015) The TAOH concentration in the experiments could be calculated on the basis of the linear relationship between the

concentration of TAOH and its fluorescence intensity at 426 nm. Since OH radical is the only reactant for the formation of TAOH, the concentration of ·OH was calculated through the formula [·OH] = [TAOH]/0.45. Fluorescence experiments result (Fig. 5) shows that signal intensity for ·OH was the highest for bio-Au_2@TiO_2. Meanwhile, the amount of ·OH produced in solution followed the order of bio-Au_2@TiO_2 > bio-Au_1@TiO_2 > bio-$Au_{0.75}$@TiO_2 > bio-$Au_{0.5}$@TiO_2 > bio-TiO_2, which is in accordance with the catalytic degradation speed of methylene blue.

In the photocatalytic process, electron-hole pairs are created by excitation of electron from valence band to the conduction band. The photogenerated electrons (e^-) and hole (h^+) pairs could react with adsorbed O_2 and H_2O to generate •OH. In the irradiation of UV light, biosynthesized TiO_2 can be photoexcited and produce electron-hole pairs to form hydroxyl radicals, thereby realizing the degradation of methylene blue (Scheme 1).

More importantly, Au NPs in bio-Au_x@TiO_2 play a vital role in the photocatalytic effect. The UV irradiation by the Au NPs resulted in the positive charges in the lower 5d band of Au, which can capture electrons from the organic pollutants adsorbed on AuNPs, ensuing in the oxidation of methylene blue. Furthermore, as Au is added to TiO_2, its band gap energy decreases below the values in anatase and rutile TiO_2. The decrease in the band gap energy of TiO_2 resulted in the stronger interaction between Au and TiO_2, and increased charge separation between the excited electron (e^-) and hole (h^+), causing the enhancement of photocatalytic activity of TiO_2. Besides, the biosynthesized materials, particularly Au NPs, are nanoscale with large specific surface area, which are capable to adsorb more methylene blue molecules, contributing to the high catalytic activity.

Thus, bio-Au_x@TiO_2 materials, especially bio-Au_2@TiO_2, displayed the superior catalytic activity in the degradation of methylene blue.

4. Conclusion

In sum, bio-TiO_2 and bio-Au_x@TiO_2 were synthesized via dehydration reaction and Au(III) bioreduction. Multiple complementary characterizations verified that IMH strain could successfully synthesize bio-TiO_2 and bio-Au_x@TiO_2 materials, and Au NPs were uniformly distributed in the bio-TiO_2 layers in the bio-Au_x@TiO_2 system. The green-synthesized bio-TiO_2 and bio-Au_x@TiO_2 exhibited elevated catalytic activity for the degradation of methylene blue. In particular, bio-Au_2@TiO_2 showed the highest *k* value of 0.195 min^{-1}. The superior catalytic activity was attributed to enhanced generation of hydroxyl radicals. The Au NPs with large surface area, adsorbed more target molecules, decreased the band gap energy of TiO_2, and increased charge separation between the excited (h^+) –(e^-) pairs, resulting in the pronounced photocatalytic activity of TiO_2. The bio-Au_x@TiO_2 material could be the promising catalytic materials, and the green synthesis provides a route to the recovery of noble metals (Au *et al.*) and synthesis of metal-semiconductor catalysts for organic pollutants degradation.

Declarations

Author Contribution

Yanan Wang: Investigation, Data curation, Writing - original draft. **Tieliang Zhang**: Methodology, Data curation, Visualization. **Yujie Zhao**: Resources, Formal analysis. **Tong Lv**: Investigation, Data curation. **Wenjing Liu:** Conceptualization, Writing - review & editing, Funding acquisition, Supervision. **Xiaowei Liu**:, Conceptualization, Resources, Funding acquisition.

Funding

Thanks for the financial support of the National Natural Science Foundation of China (No. 41907291) and Central Public-interest Scientific Institution Basal Research Fund (No. 2022-jbkyywf-lwj).

Data availability

All data generated or analyzed during this study are included in this published article.

Ethics approval This article does not contain any studies with human participants or animals performed by any of the authors.

Consent to participate Not applicable.

Consent for publication Not applicable.

Competing interests The authors declare that they have no known competing financial interests or personal relationships that could have appeared to influence the work reported in this paper.

References

1. Alsaidi M, Azeez FA, Al-Hajji LA, Ismail AA (2022) Impact of reaction parameters for photodegradation pharmaceuticals in wastewater over gold/titania photocatalyst synthesized by pyrolysis of NH2-MIL-125(Ti). J Environ Manage 314:115047
2. Angthararuk D, Sutthivaiyakit P, Blaise C, Gagne F, Sutthivaiyakit S (2015) Photo-catalysis of bromacil under simulated solar light using Au/TiO2: evaluation of main degradation products and toxicity implications. Environ Sci Pollut Res Int 22:1468–1479
3. Ayati A, Ahmadpour A, Bamoharram FF, Tanhaei B, Manttari M, Sillanpaa M (2014) A review on catalytic applications of Au/TiO2 nanoparticles in the removal of water pollutant. Chemosphere 107:163–174
4. Bhargava A, Jain N, Khan MA, Pareek V, Dilip RV, Panwar J (2016) Utilizing metal tolerance potential of soil fungus for efficient synthesis of gold nanoparticles with superior catalytic activity for degradation of rhodamine B. J Environ Manage 183:22–32

5. Bosch A, Miñán A, Vescina C, Degrossi J, Gatti B, Montanaro P, Messina M, Franco M, Vay C, Schmitt J, Naumann D, Yantorno O (2008) Fourier transform infrared spectroscopy for rapid identification of nonfermenting gram-negative bacteria isolated from sputum samples from cystic fibrosis patients. J Clin Microbiol 46:2535–2546
6. Cai J, Niu B, Xie Q, Lu N, Huang S, Zhao G, Zhao J (2022) Accurate Removal of Toxic Organic Pollutants from Complex Water Matrices. Environ Sci Technol 56:2917–2935
7. Chen C, Ma W, Zhao J (2010) Semiconductor-mediated photodegradation of pollutants under visible-light irradiation. Chem Soc Rev 39:4206–4219
8. Chen X, Mao SS (2007) Titanium dioxide nanomaterials: Synthesis, properties, modifications, and applications. Chem Rev 107:2891–2959
9. Chong MN, Jin B, Chow CWK, Saint C (2010) Recent developments in photocatalytic water treatment technology: A review. Water Res 44:2997–3027
10. Dahl JA, Maddux BLS, Hutchison JE (2007) Toward greener nanosynthesis. Chem Rev 107:2228–2269
11. Dawson A, Kamat PV (2001) Semiconductor – Metal Nanocomposites. Photoinduced Fusion and Photocatalysis of Gold-Capped TiO2 (TiO2/Gold) Nanoparticles. J Phys Chem B 105:960–966
12. de Luna LAV, da Silva THG, Pupo Nogueira RF, Kummrow F, Umbuzeiro GA (2014) Aquatic toxicity of dyes before and after photo-Fenton treatment. J Hazard Mater 276:332–338
13. Fischer G, Braun S, Thissen R, Dott W (2006) FT-IR spectroscopy as a tool for rapid identification and intra-species characterization of airborne filamentous fungi. J Microbiol Meth 64:63–77
14. Forgacs E, Cserhati T, Oros G (2004) Removal of synthetic dyes from wastewaters: a review. Environ Int 30:953–971
15. Green IX, Tang W, Neurock M, Yates JT Jr (2014) Insights into Catalytic Oxidation at the Au/TiO2 Dual Perimeter Sites. Acc Chem Res 47:805–815
16. Khalid NR, Ahmed E, Ahmad M, Niaz NA, Ramzan M, Shakil M, Iqbal T, Majid A (2016) Microwave-assisted synthesis of Ag–TiO2/graphene composite for hydrogen production under visible light irradiation. Ceram Int 42:18257–18263
17. Kochuveedu ST, Jang YH, Kim DH (2013) A study on the mechanism for the interaction of light with noble metal-metal oxide semiconductor nanostructures for various photophysical applications. Chem Soc Rev 42:8467–8493
18. Lee KM, Lai CW, Ngai KS, Juan JC (2016) Recent developments of zinc oxide based photocatalyst in water treatment technology: A review. Water Res 88:428–448
19. Lengke MF, Ravel B, Fleet ME, Wanger G, Gordon RA, Southam G (2006) Mechanisms of gold bioaccumulation by filamentous cyanobacteria from gold(III) - Chloride complex. Environ Sci Technol 40:6304–6309
20. Li H, Liang L, Niu X, Zhang D, Fan H, Wang K (2022) Construction of a Bi2WO6/TiO2 heterojunction and its photocatalytic degradation performance. New J. Chem

21. Liang W, Church TL, Harris AT (2012) Biogenic synthesis of photocatalytically active Ag/TiO2 and Au/TiO2 composites. Green Chem 14:968–975
22. Liu L, Corma A (2018) Metal Catalysts for Heterogeneous Catalysis: From Single Atoms to Nanoclusters and Nanoparticles. Chem Rev 118:4981–5079
23. Liu LC, Gu XR, Cao Y, Yao XJ, Zhang L, Tang CJ, Gao F, Dong L (2013) Crystal-Plane Effects on the Catalytic Properties of Au/TiO2. ACS Catal 3:2768–2775
24. Liu W, Wang L, Wang J, Du J, Jing C (2018a) New insights into microbial-mediated synthesis of Au@biolayer nanoparticles. Environ Sci -Nano 5:1757–1763
25. Liu W, Wang Y, Jing C (2018b) Transcriptome analysis of silver, palladium, and selenium stresses in Pantoea sp. IMH Chemosphere 208:50–58
26. Miranda LDL, Bellato CR, Milagres JL, Moura LG, Mounteer AH, de Almeida MF (2015) Hydrotalcite-TiO2 magnetic iron oxide intercalated with the anionic surfactant dodecylsulfate in the photocatalytic degradation of methylene blue dye. J Environ Manage 156:225–235
27. Nakabayashi Y, Nosaka Y (2015) The pH dependence of OH radical formation in photo-electrochemical water oxidation with rutile TiO2 single crystals. Phys Chem Chem Phys 17:30570–30576
28. Nasrollahzadeh M, Sajadi SM (2016) Green synthesis, characterization and catalytic activity of the Pd/TiO2 nanoparticles for the ligand-free Suzuki-Miyaura coupling reaction. J Colloid Interf Sci 465:121–127
29. Nasrollahzadeh M, Sajjadi M, Dadashi J, Ghafuri H (2020) : Pd-based nanoparticles: Plant-assisted biosynthesis, characterization, mechanism, stability, catalytic and antimicrobial activities.Adv. Colloid. Interface. Sci.276
30. Nassar MY, Ali AA, Amin AS (2017) A facile Pechini sol–gel synthesis of TiO2/Zn2TiO2/ZnO/C nanocomposite: an efficient catalyst for the photocatalytic degradation of Orange G textile dye. RSC Adv 7:30411–30421
31. Ni Z, Zeng X, Li X, Xia G, Luo S, Zhang Y (2021) Simple preparation of nano-anatase titanium dioxide from cold rolled titanic acid waste liquid. Ionics 27:2119–2126
32. Pelaez M, Nolan NT, Pillai SC, Seery MK, Falaras P, Kontos AG, Dunlop PSM, Hamilton JWJ, Byrne JA, O'Shea K, Entezari MH, Dionysiou DD (2012) A review on the visible light active titanium dioxide photocatalysts for environmental applications. Appl Catal B-Environ 125:331–349
33. Reith F, Rogers SL, McPhail DC, Webb D (2006) Biomineralization of gold: Biofilms on bacterioform gold. Science 313:233–236
34. Routoula E, Patwardhan SV (2020) Degradation of Anthraquinone Dyes from Effluents: A Review Focusing on Enzymatic Dye Degradation with Industrial Potential. Environ Sci Technol 54:647–664
35. Saeed M, Muneer M, Haq Au, Akram N (2022) Photocatalysis: an effective tool for photodegradation of dyes-a review. Environ Sci Pollut Res Int 29:293–311
36. Sahu A, Singh P, Singh P, Gahlot APS, Mehrotra R, Inorg (2022)Nano-Met. Chem

37. Sanyal SK, Shuster J, Reith F (2019) : Biogeochemical gold cycling selects metal-resistant bacteria that promote gold particle transformation.FEMS Microbiol. Ecol.95
38. Sarina S, Waclawik ER, Zhu H (2013) Photocatalysis on supported gold and silver nanoparticles under ultraviolet and visible light irradiation. Green Chem 15:1814–1833
39. Schmitt J, Flemming H-C (1998) FTIR-spectroscopy in microbial and material analysis. Int Biodeter Biodegr 41:1–11
40. Singh P, Kim Y-J, Zhang D, Yang D-C (2016) Biological Synthesis of Nanoparticles from Plants and Microorganisms. Trends Biotechnol 34:588–599
41. Southam G, Lengke MF, Fairbrother L, Reith F (2009) The Biogeochemistry of Gold. Elements 5:303–307
42. Tran NM, Kim S, Yoo H (2022) Gold nanodot assembly within a cobalt chalcogenide nanoshell: Promotion of electrocatalytic activity. J Colloid Interf Sci 605:274–285
43. Trino LD, Bronze-Uhle ES, George A, Mathew MT, Lisboa-Filho PN (2018) Surface Physicochemical and Structural Analysis of Functionalized Titanium Dioxide Films. Colloid Surf A 546:168–178
44. Zhang N, Liu S, Xu Y-J (2012) Recent progress on metal core@semiconductor shell nanocomposites as a promising type of photocatalyst. Nanoscale 4:2227–2238
45. Zou Y, Gong Y, Lin B, Mellott NP (2016) Photodegradation of methylene blue in the visible spectrum: An efficient W6 + ion doped anatase titania photocatalyst via a solvothermal method. Vacuum 126:63–69

Schemes

Scheme 1 is available in the Supplementary Files section

Figures

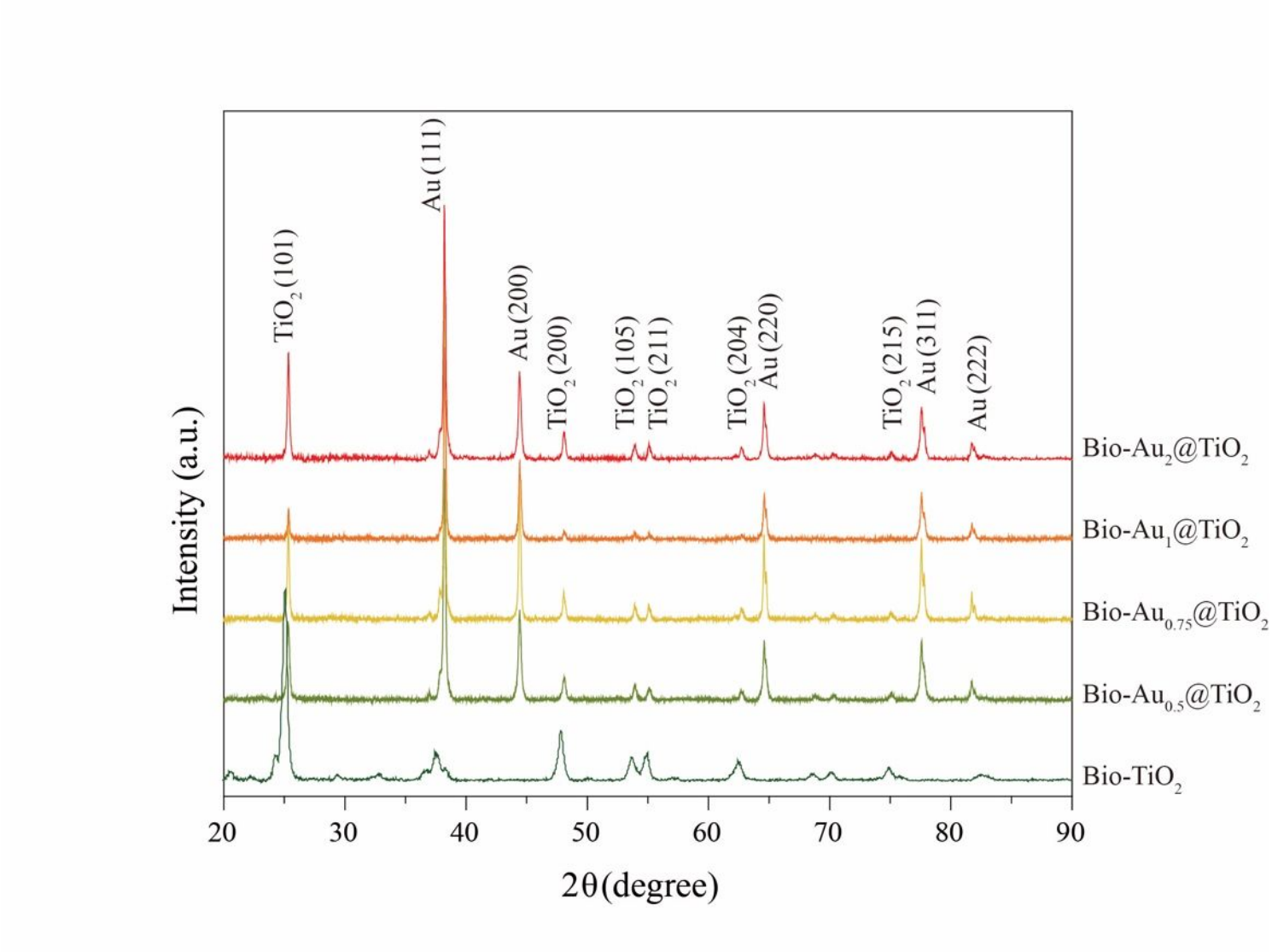

Figure 1

XRD patterns of bio-TiO_2 and bio-Au_x@TiO_2 samples.

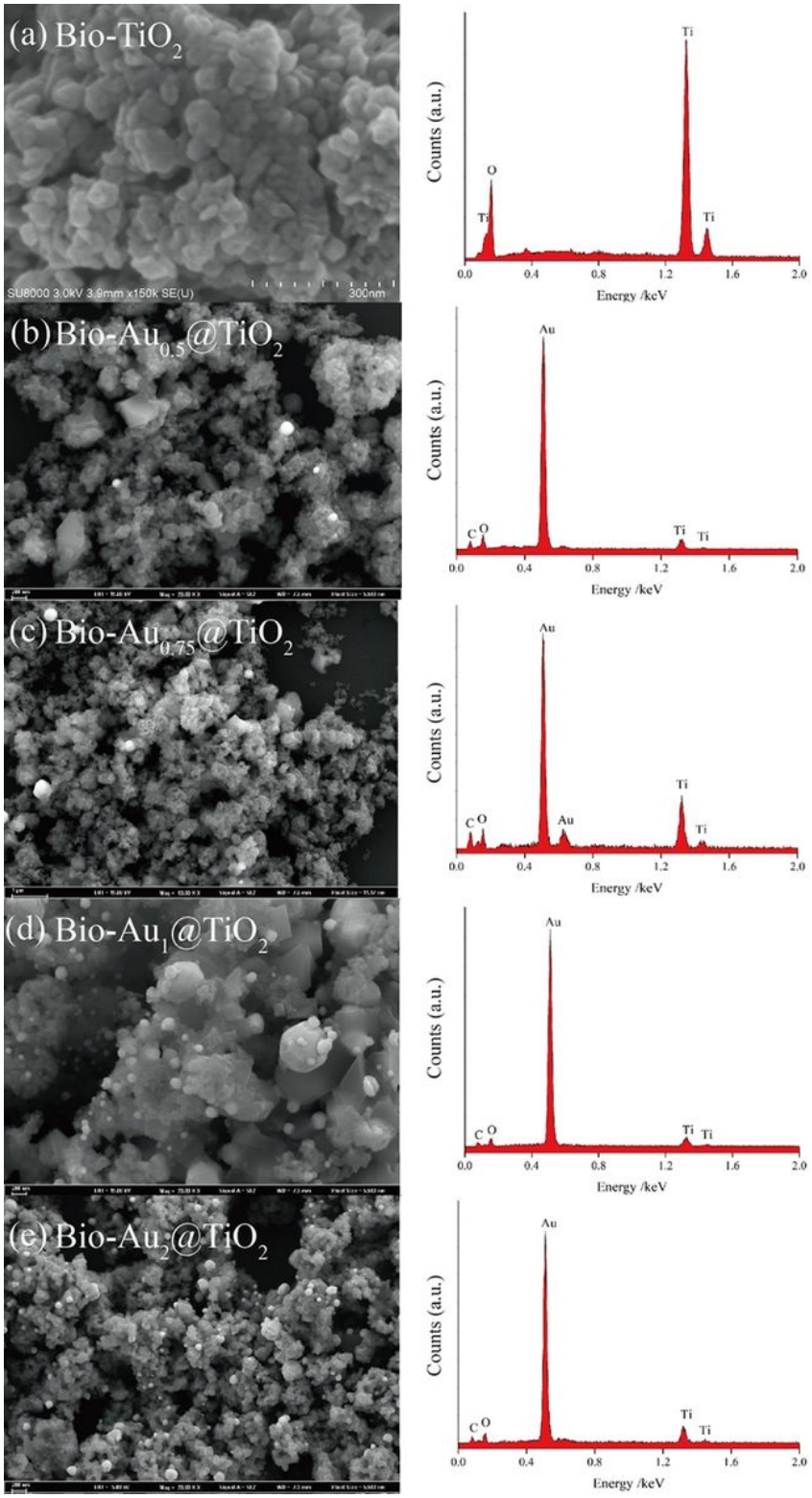

Figure 2

FE-SEM micrographs and EDX spectra of bio-TiO_2 and bio-Au_x@TiO_2 nanocomposite.

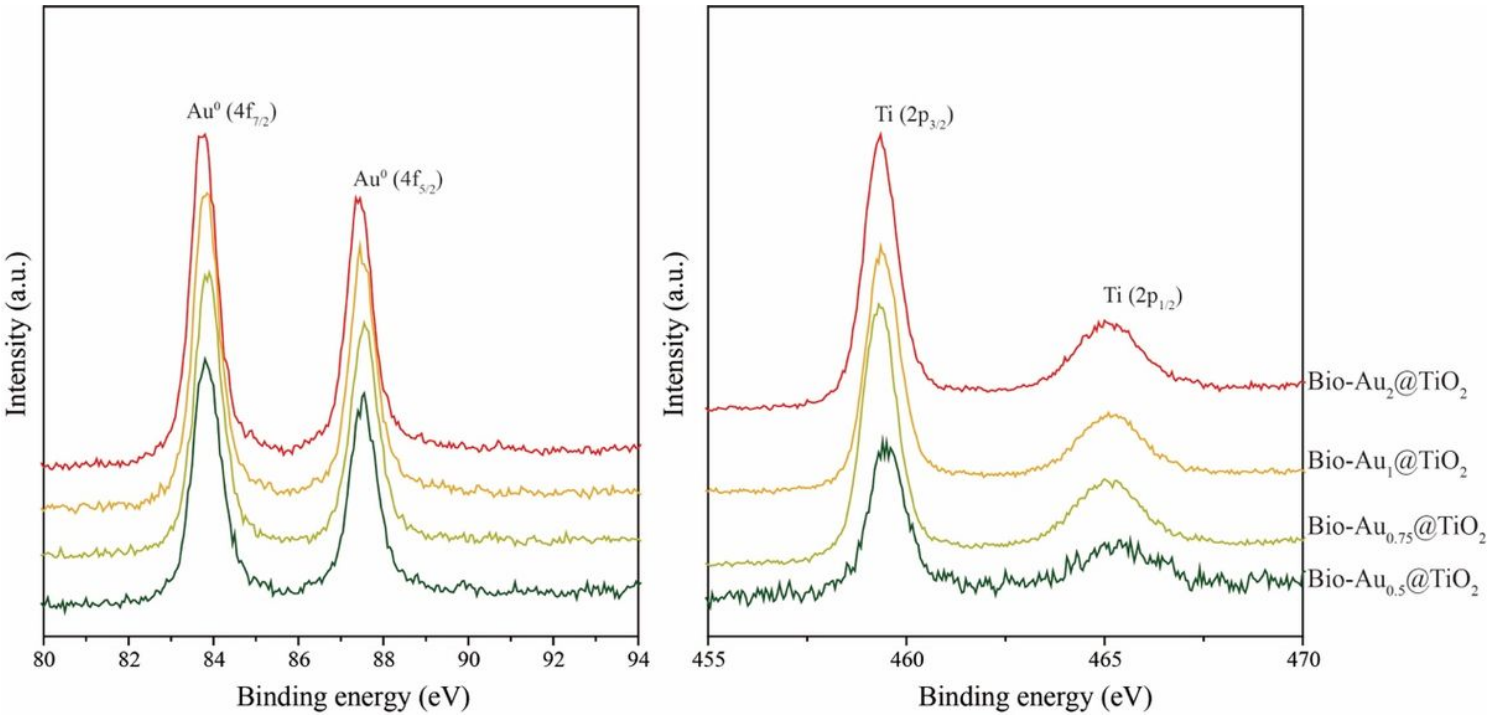

Figure 3

XPS survey spectra of Au and Ti in bio-Au_x@TiO_2.

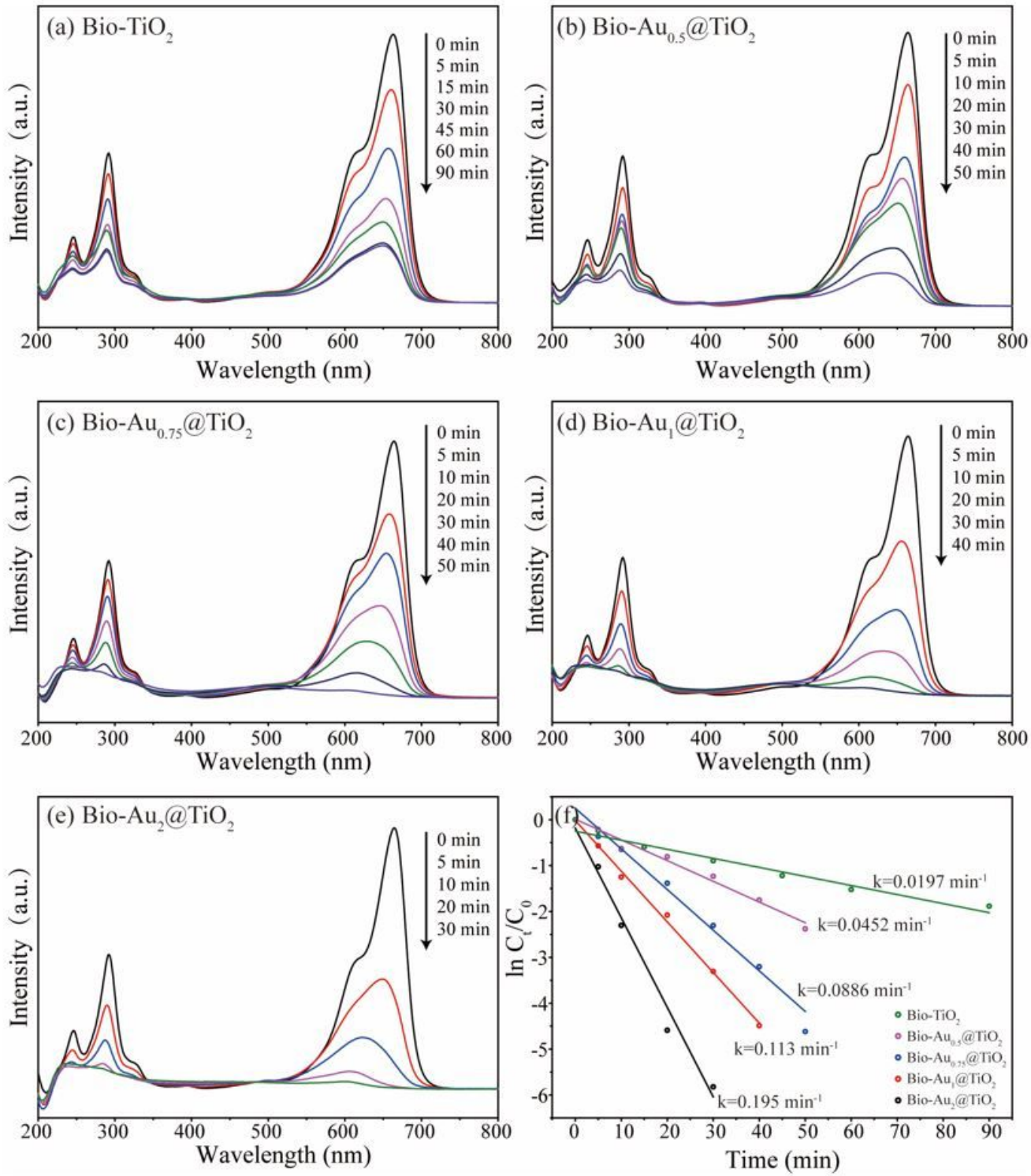

Figure 4

UV-Vis absorption spectra showing the degradation of methylene blue by bio-TiO_2 (a), bio-$Au_{0.5}$@TiO_2 (b), bio-$Au_{0.75}$@TiO_2 (c), bio-Au_1@TiO_2 (d) and bio-Au_2@TiO_2 (e); and Plot of $\ln(C_t/C_0)$ against the reaction time for the degradation of methylene blue by bio-TiO_2 and bio-Au_x@TiO_2 materials (f). k represents the value of k_{app}.

Figure 5

The production of •OH in the bio-TiO_2 and bio-Au_x@TiO_2 materials at different UV irradiation times.

Supplementary Files

This is a list of supplementary files associated with this preprint. Click to download.

- TOCGraphic.jpg
- Scheme1.jpg
- SupplementaryInformation0617.docx